VIP Photochemistry Very Important Paper

Deutsche Ausgabe: DOI: 10.1002/ange.201510503
Internationale Ausgabe: DOI: 10.1002/anie.201510503

Light-Harvesting Systems Based on Organic Nanocrystals To Mimic Chlorosomes

*Peng-Zhong Chen, Yu-Xiang Weng, Li-Ya Niu, Yu-Zhe Chen, Li-Zhu Wu, Chen-Ho Tung, and Qing-Zheng Yang**

Abstract: *We report the first highly efficient artificial light-harvesting systems based on nanocrystals of difluoroboron chromophores to mimic the chlorosomes, one of the most efficient light-harvesting systems found in green photosynthetic bacteria. Uniform nanocrystals with controlled donor/acceptor ratios were prepared by simple coassembly of the donors and acceptors in water. The light-harvesting system funneled the excitation energy collected by a thousand donor chromophores to a single acceptor. The well-defined spatial organization of individual chromophores in the nanocrystals enabled an energy transfer efficiency of 95 %, even at a donor/acceptor ratio as high as 1000:1, and a significant fluorescence of the acceptor was observed up to donor/acceptor ratios of 200 000:1.*

In plants and bacteria, photosynthesis usually starts with the absorption of sunlight by antenna chromophores in light-harvesting systems, followed by the highly efficient transfer of the excitation energy to an acceptor of the reaction center.[1] In bacteria, over 200 bacteriochlorophylls supply energy to one chromophore of the reaction center with an efficiency of over 95 %.[1,2] This high efficiency is possible because of the well-organized arrays of chromophores in the photosynthetic membrane.[1a] Considerable effort has been devoted to mimic this light-harvesting process, because of both its role in photosynthesis and its potential significance to photocatalysis, solar cells, optical sensors, and luminescent materials.[3]

Although impressive examples of artificial light-harvesting systems constructed using both covalent and noncovalent interactions have been reported,[4–8] their light-harvesting capacity remains a fraction of that of the natural counterparts. An artificial light-harvesting with a high energy collection efficiency should have the following two properties, namely, 1) contain multiple antenna chromophores per acceptor and 2) transfer the excitation energy with high efficiency. Artificial light-harvesting systems constructed with covalent bonds, such as porphyrin arrays and dendrimers, contain very few donor chromophores per acceptor because of synthetic difficulties. Self-assembled light-harvesting systems, such as organic gels, biopolymer assemblies, and organic–inorganic hybrid materials, have high donor/acceptor ratios, but low energy-transfer efficiencies probably because of the low degree of spatial organization of the chromophores.

The chlorosomes, one of the most efficient light-harvesting systems found in green photosynthetic bacteria, contains large numbers of bacteriochlorophyll molecules organized in stacked structures through self-assembly without any direct involvement of proteins. Interaction between chromophores within the chlorosomes lead to the formation of delocalized electronic excitations, that is, excitons, which facilitate its high energy-collection efficiency.[9] However, studies focusing on mimicking the chlorosomes are still rare.[10] Herein, we prepared light-harvesting systems based on organic nanocrystals. Organic nanocrystals of chromophores containing multiple chromophores in well-defined relative orientations and distances may provide an ideal scaffold for artificial light-harvesting systems. Such nanocrystals have attracted much attention recently because of their promising applications in electronic and photonic devices.[11] However, to the best of our knowledge, no examples of light-harvesting antenna systems based on nanocrystals of chromophores have been reported. We describe two such systems that were fabricated by coassembly of the donor and acceptor chromophores at molar ratios ranging from 1×10^6:1 to 1000:1. High energy-transfer efficiency (95 %) was observed even for the nanocrystals with a donor/acceptor ratio of 1000:1.

We chose the difluoroboron β-diketonate (BF_2dbk) derivative BF_2bcz as our model antenna chromophore, because of its high fluorescence in both solution and the solid state. BF_2cna or BF_2dan, analogues of BF_2bcz, were used as the energy acceptor (Figure 1). The three BF_2dbk derivatives were synthesized in approximately 70 % yield by Claisen condensation of the corresponding acetophenones with benzoates, followed by treatment with BF_3/Et_2O (see the Supporting Information). BF_2bcz is a typical donor–acceptor–donor (D-A-D) type fluorophore, with the difluoroboron moiety acting as the electron acceptor and the amino group of the carbazole acting as the electron donor. It has been reported that a donor–acceptor dipole–dipole interaction between two adjacent molecules can guide the preferential

---

[*] Dr. P.-Z. Chen, Dr. L.-Y. Niu, Prof. Dr. Q.-Z. Yang
Key Laboratory of Radiopharmaceuticals
Ministry of Education, College of Chemistry
Beijing Normal University, Beijing 100875 (China)
E-mail: qzyang@bnu.edu.cn

Prof. Dr. Y.-X. Weng
Key Laboratory of Soft Matter physics
Institute of Physics, Chinese Academy of Sciences
Beijing 100190 (China)

Dr. P.-Z. Chen, Dr. L.-Y. Niu, Dr. Y.-Z. Chen, Prof. Dr. L.-Z. Wu,
Prof. Dr. C.-H. Tung, Prof. Dr. Q.-Z. Yang
Key Laboratory of Photochemical Conversion and
Optoelectronic Materials
Technical Institute of Physics and Chemistry
Chinese Academy of Sciences
Beijing 100190 (China)

Supporting information for this article is available on the WWW under http://dx.doi.org/10.1002/anie.201510503.

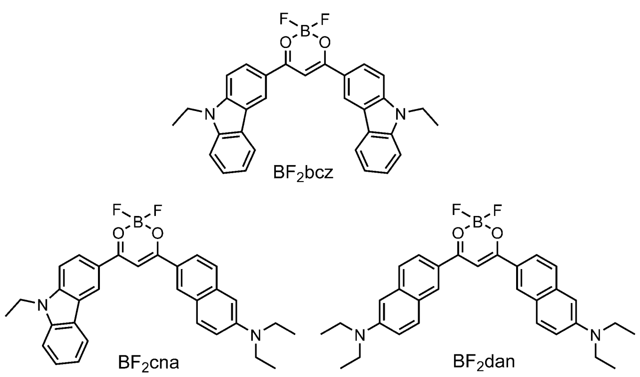

Figure 1. The molecular structures of BF$_2$bcz, BF$_2$cna, and BF$_2$dan.

growth of 1D or semi-1D nanostructures.[12] X-ray crystallographic analysis of a single crystal of BF$_2$bcz grown from chloroform showed that the BF$_2$bcz molecule was nearly planar and aggregated in a slipped-stack geometry directed by the intermolecular CH⋯π interaction and CH⋯F hydrogen bonding (Figure S3 in Supporting Information). The structural properties of BF$_2$bcz facilitated its assembly into nanocrystals by a template-assisted assembly method in water in the presence of sodium dodecyl sulfate (SDS; see Figures S1 and S2 in the Supporting Information). Figure 2 a,b displays the typical scanning electron microscopy (SEM) and transmission electron microscopy (TEM) images of as-prepared BF$_2$bcz nanocrystals, which have a smooth surface and uniform size with a width of 500–600 nm and a length of about 7 μm. Both anionic (e.g. SDS or sodium dodecyl benzene sulfonate) and cationic surfactants (e.g. hexadecyl trimethyl ammonium bromide) yielded 1D crystalline BF$_2$bcz nanorods of uniform morphology (Figure S4 in the Supporting Information).

We prepared the light-harvesting systems by coassembly of BF$_2$bcz and different amounts of the BF$_2$dan or BF$_2$cna acceptors in water, with SDS as the surfactant. The amount of dopant (0.0001–0.1 mol %) did not influence the morphology and monodispersity of the nanocrystals (Figure 2 c,d and see Figure S5 in the Supporting Information). To further investigate the crystal structure of the nanocrystals, we measured the X-ray diffraction (XRD) patterns of the nanocrystals without dopant and with a doping ratio of 0.1 mol %. Compared with the X-ray diffraction pattern of the bulk crystal of BF$_2$bcz, the diffraction peaks of (202) lattice planes were weakened greatly for nanocrystals, while the peaks of (110) lattice planes were strengthened significantly (Figure S6 in the Supporting Information). This finding indicates that these nanocrystals grew preferentially along the [110] direction (Figure S7 in the Supporting Information). The (110) and (220) diffraction peaks, which correspond to a d spacing of 1.16 nm and 0.58 nm, respectively, indicated a lamellar structure within the nanocrystals with an interlayer distance of 1.16 nm. At a doping ratio of 0.1 mol %, the doped nanocrystals showed identical XRD patterns to that of pure BF$_2$bcz nanocrystals. This result indicates that doping small amounts of BF$_2$dan or BF$_2$cna did not change the crystallinity of the nanocrystals, probably because of the structural similarity of the three molecules enabling simple replacement of the BF$_2$bcz molecules by the acceptor in its crystal lattice.

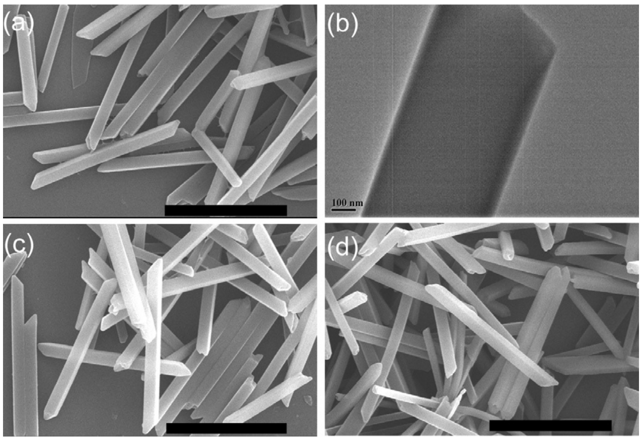

Figure 2. a) SEM and b) TEM images of as-prepared BF$_2$bcz nanocrystals obtained by SDS-assisted reprecipitation at room temperature. c,d) SEM images of BF$_2$bcz nanocrystals doped with 0.1 mol % BF$_2$dan and BF$_2$cna, respectively, prepared under the same conditions as that in (a). Scale bar in SEM images: 5 μm.

BF$_2$bcz showed green fluorescence in CH_2Cl_2. In contrast, the emission bands of BF$_2$cna and BF$_2$dan in CH_2Cl_2 were located in the red region because of the more predominant electron-donating capability of the amino group of the naphthalene units compared with the carbazole units (Figure S8 in the Supporting Information). Aqueous dispersions of BF$_2$bcz nanocrystals had a strong yellow fluorescence with an emission band centered at $\lambda = 567$ nm when excited at 480 nm, and thus is red-shifted by about 50 nm compared with that of the monomer in CH_2Cl_2 (Figure S9 in the Supporting Information). Intermolecular dipole–dipole interactions and π-π stacking between BF$_2$bcz molecules are the possible reasons for the red-shift. The absorption spectra of BF$_2$cna or BF$_2$dan showed good overlap with the emission spectra of the BF$_2$bcz nanocrystals (Figure S10 in the Supporting Information).

Energy transfer from the BF$_2$bcz to BF$_2$cna or BF$_2$dan in the nanocrystals was confirmed by steady-state and time-resolved fluorescence spectroscopy. Significant changes in the fluorescence were observed with nanocrystals containing different amounts of BF$_2$cna or BF$_2$dan. As shown in Figure 3 a,b, increasing the concentration of the doped acceptor decreased the intensity of the donor emission centered at $\lambda =$ 567 nm, with a simultaneous growth of new emission bands at $\lambda = 616$ nm or $\lambda = 636$ nm, which we ascribed to the emission of BF$_2$cna or BF$_2$dan, respectively. When the molar ratio of the acceptor reached 0.1 mol % relative to BF$_2$bcz, the donor emission was almost completely quenched and only acceptor emission was observed. Remarkably, a significant fluorescence of the acceptor was observed even at extremely high donor/acceptor ratios (up to 200 000:1), thus illustrating the highly efficient energy transfer in these nanocrystals. Time-resolved fluorescence measurements revealed a remarkable decrease in the donor fluorescence lifetime (τ) upon increasing the acceptor/donor ratios (Figure 3 c,d; see also Figure S11 and Table S1 in the Supporting Information), which

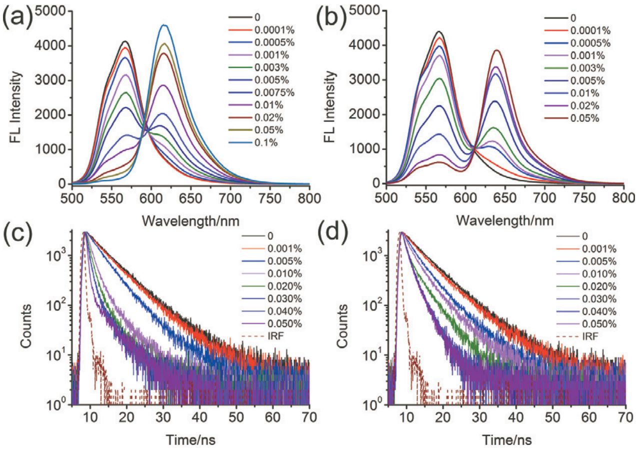

Figure 3. a,b) Fluorescence spectra of aqueous dispersions of BF_2bcz nanocrystals doped with different amounts of BF_2cna (a) and BF_2dan (b), $\lambda_{ex} = 480$ nm. c,d) Lifetime decay profiles of the aqueous dispersion of BF_2bcz nanocrystals containing different amounts of BF_2cna (c) and BF_2dan (d) monitored at $\lambda = 540$ nm. IRF = instrument response function.

demonstrates the occurrence of efficient energy transfer from the donors to the doped acceptors in the nanocrystals.

The energy transfer was also apparent by the variation in the emission color of aqueous dispersions of nanocrystals doped with different amounts of acceptor under illumination with a UV lamp (Figure 4a and see Figure S12a in the Supporting Information). In the absence of the acceptor, aqueous dispersions of BF_2bcz nanocrystals exhibited yellow fluorescence. The fluorescence color changed to orange and red on increasing the amounts of BF_2dan or BF_2cna. The variation in the macroscopic color was also observed in individual nanocrystals doped with different amounts of acceptor molecules by microscopy imaging (Figure 4b and Figure S12b in the Supporting Information), further indicating the efficient energy transfer. In addition, every nanocrystal in all the samples had a homogeneous emission color, thus confirming that the acceptor molecules were dispersed uniformly in the BF_2bcz matrix.

In control experiments, no energy transfer was observed in solutions of the donor and the acceptor at a molar ratio of 0.1 mol% in CH_2Cl_2. The emission spectra of such solutions upon excitation at $\lambda = 480$ nm were dominated by that of pure BF_2bcz (Figure S13 in the Supporting Information). Moreover, the efficiency of the energy transfer was much lower (less than 30%) for the the BF_2bz nanocrystals that adsorbed 0.1 mol% of the acceptors on their surfaces compared with that of the cocrystalline systems (Figure S14 in the Supporting Information). These results confirmed that well-defined intermolecular organization of the donor and the acceptor in nanocrystals is essential for efficient energy transfer.

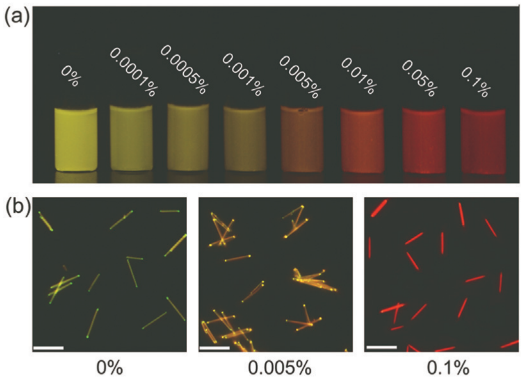

Figure 4. a) Fluorescence images of aqueous dispersions of nanocrystals doped with different amounts of BF_2dan. b) Fluorescence microscopy images of nanocrystals doped with different amounts of BF_2dan. Scale bar: 5 μm.

The strong intermolecular coupling in our light-harvesting systems may result in the excitation energy being delocalized over more than one molecule.[1d] An exciton transfer (i.e. coherent resonance energy transfer) mechanism could be expected in such systems, as displayed schematically in Figure 5a.[1e,13] The exciton is formed upon irradiation of the nanocrystals. The resonant excitonic structure could result in very rapid migration of the exciton throughout the coupled chromophore aggregates, with the excitation energy finally being funneled efficiently to the acceptor.[14] Since the intermolecular interaction is strong within a layer of nanocrystals having a lamellar structure, the migration of the exciton within the layers is expected to be more efficient than that between the layers. By plotting $1/\tau$ against the concentration of the acceptors, the exciton migration rate constants were estimated to be on the order of $10^{12}\,\mathrm{M}^{-1}\mathrm{s}^{-1}$, which indicates that the migration rate of excitonic energy within the nanocrystal is much larger than the diffusion limit for the bimolecular reaction in solution (Figure 5 and Figure S15 in the Supporting Information).[14f,15] The efficiency of the energy transfer was 95% with BF_2cna as dopants and 90% with BF_2dan as dopants at a doping ratio of 0.1 mol% (Figure S16 in the Supporting Information), thus indicating

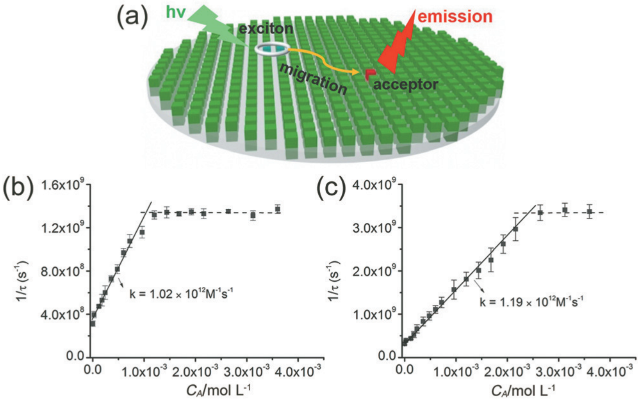

Figure 5. a) Schematic representation of a section of the self-assembled nanocrystal, which contains a large number of donors and only a few acceptors. Initially the excitation energy is delocalized over many donor molecules, and then transferred to acceptors mainly through exciton migration pathways. c,d) Plots of the reciprocal of the lifetime of the BF_2bcz nanocrystals containing different concentrations of BF_2dan (b) and BF_2cna (c) monitored at $\lambda = 540$ nm against the concentrations of the acceptors. The slope gives the corresponding second-order rate constant (k) for the exciton migration towards the acceptor.

that the excitation energy absorbed by approximately 1000 donors was efficiently funneled to a single acceptor. Furthermore, the estimated donor/acceptor ratio of 1000:1, which achieved a high energy transfer efficiency (over 90%), is much higher than those of previously reported light-harvesting systems such as self-assembled [*n*]acene gel fibers (200:1 with $\Phi_{ET} = 35\,\%$)[5a] and amphiphilic naphthalene soft nanotubes with anthracene as the acceptor in the nanochannels (20:1 with $\Phi_{ET} = 40\,\%$).[5d]

The light-harvesting capacity was quantified as the antenna effect, a widely used empirical parameter to determine the degree of amplified emission resulting from excitation of the donor. In our system, the antenna effect $= I_{A,370}/I_{A,555}$, where $I_{A,370}$ and $I_{A,555}$ are the fluorescence intensities of the acceptor upon excitation of the donor at $\lambda = 370$ nm and upon direct excitation of the acceptor at $\lambda = 555$ nm, respectively. The maximum acceptor emission amplification factors were 28 and 29 for BF_2cna and BF_2dan, respectively (Figure S17 in the Supporting Information) at a doping concentration of 0.01 mol%. It further demonstrated that such nanocrystals functioned as an excellent light-harvesting antenna.

In conclusion, we have described highly efficient light-harvesting antenna systems based on nanocrystals of organic chromophores to mimic chlorosomes for the first time. A simple coassembly approach in aqueous solution was employed to achieve uniform nanocrystals with controlled donor/acceptor ratios. The highly ordered arrangement of the chromophores resulted in extremely efficient energy transfer. The light-harvesting system funneled the excitation energy of a thousand donor chromophores to a single acceptor, which is the highest donor/acceptor ratio reported in the literature. The highly efficient energy transfer and simple preparation of such light-harvesting systems make them potentially useful in photocatalysis, light-emitting devices, and optical sensors, and our strategy may inspire the exploration of novel light-harvesting systems based on organic nanocrystals. We are currently using ultrafast spectroscopy to understand the mechanism of the exciton transport in our light-harvesting system.

Acknowledgements

This work was financially supported by the 973 program (2013CB834800, 2013CB933800), National Natural Science Foundation of China (21525206, 21222210, 21472202), the Fundamental Research Funds for the Central Universities, and Beijing Municipal Commission of Education. Y.-Z.C. thanks the NSFC (21272243) for partial support of the research. We thank the referees for their thoughtful suggestions to improve our work.

Keywords: chlorosomes · exciton migration · light harvesting · nanostructures · self-assembly

How to cite: *Angew. Chem. Int. Ed.* **2016**, *55*, 2759–2763
Angew. Chem. **2016**, *128*, 2809–2813

[1] a) G. McDermott, S. M. Prince, A. A. Freer, A. M. Hawthornthwaite-lawless, M. Z. Papiz, R. J. Cogdell, N. W. Isaacs, *Nature* **1995**, *374*, 517–521; b) X. C. Hu, A. Damjanovic, T. Ritz, K. Schulten, *Proc. Natl. Acad. Sci. USA* **1998**, *95*, 5935–5941; c) A. M. van Oijen, M. Ketelaars, J. Kohler, T. J. Aartsma, J. Schmidt, *Science* **1999**, *285*, 400–402; d) R. J. Cogdell, A. Gall, J. Kohler, *Q. Rev. Biophys.* **2006**, *39*, 227–324; e) R. M. Clegg, M. Sener, Govindjee, *Proc. SPIE-Int. Soc. Opt. Eng.* **2010**, *7561*, 75610C; f) G. D. Scholes, G. R. Fleming, A. Olaya-Castro, R. van Grondelle, *Nat. Chem.* **2011**, *3*, 763–774.

[2] a) R. A. Miller, A. D. Presley, M. B. Francis, *J. Am. Chem. Soc.* **2007**, *129*, 3104–3109; b) J. Chmeliov, G. Trinkunas, H. van Amerongen, L. Valkunas, *J. Am. Chem. Soc.* **2014**, *136*, 8963–8972.

[3] a) D. T. McQuade, A. H. Hegedus, T. M. Swager, *J. Am. Chem. Soc.* **2000**, *122*, 12389–12390; b) D. Gust, T. A. Moore, A. L. Moore, *Acc. Chem. Res.* **2001**, *34*, 40–48; c) T. Mayr, S. M. Borisov, T. Abel, B. Enko, K. Waich, G. Mistlberger, I. Klimant, *Anal. Chem.* **2009**, *81*, 6541–6545; d) P. Duan, N. Yanai, H. Nagatomi, N. Kimizuka, *J. Am. Chem. Soc.* **2015**, *137*, 1887–1894; e) F. Pu, L. Wu, X. Ran, J. Ren, X. Qu, *Angew. Chem. Int. Ed.* **2015**, *54*, 892–896; *Angew. Chem.* **2015**, *127*, 906–910.

[4] a) K. Becker, J. M. Lupton, *J. Am. Chem. Soc.* **2006**, *128*, 6468–6479; b) R. Ziessel, G. Ulrich, A. Haefele, A. Harriman, *J. Am. Chem. Soc.* **2013**, *135*, 11330–11344; c) Y. H. Jeong, M. Son, H. Yoon, P. Kim, D. H. Lee, D. Kim, W. D. Jang, *Angew. Chem. Int. Ed.* **2014**, *53*, 6925–6928; *Angew. Chem.* **2014**, *126*, 7045–7048.

[5] a) A. Del Guerzo, A. G. L. Olive, J. Reichwagen, H. Hopf, J.-P. Desvergne, *J. Am. Chem. Soc.* **2005**, *127*, 17984–17985; b) A. Ajayaghosh, V. K. Praveen, C. Vijayakumar, S. J. George, *Angew. Chem. Int. Ed.* **2007**, *46*, 6260–6265; *Angew. Chem.* **2007**, *119*, 6376–6381; c) K. V. Rao, K. K. Datta, M. Eswaramoorthy, S. J. George, *Angew. Chem. Int. Ed.* **2011**, *50*, 1179–1184; *Angew. Chem.* **2011**, *123*, 1211–1216; d) N. Kameta, K. Ishikawa, M. Masuda, M. Asakawa, T. Shimizu, *Chem. Mater.* **2012**, *24*, 209–214.

[6] a) F. Garo, R. Haner, *Angew. Chem. Int. Ed.* **2012**, *51*, 916–919; *Angew. Chem.* **2012**, *124*, 940–943; b) C. M. Spillmann, I. L. Medintz, *J. Photochem. Photobiol. C* **2015**, *23*, 1–24.

[7] a) X. Zhang, M. A. Ballem, Z. J. Hu, P. Bergman, K. Uvdal, *Angew. Chem. Int. Ed.* **2011**, *50*, 5729–5733; *Angew. Chem.* **2011**, *123*, 5847–5851; b) V. M. Suresh, S. J. George, T. K. Maji, *Adv. Funct. Mater.* **2013**, *23*, 5585–5590; c) S. Jin, H. J. Son, O. K. Farha, G. P. Wiederrecht, J. T. Hupp, *J. Am. Chem. Soc.* **2013**, *135*, 955–958; d) L. Grösch, Y. J. Lee, F. Hoffmann, M. Froba, *Chem. Eur. J.* **2015**, *21*, 331–346.

[8] a) H.-Q. Peng, Y.-Z. Chen, Y. Zhao, Q.-Z. Yang, L.-Z. Wu, C.-H. Tung, L.-P. Zhang, Q.-X. Tong, *Angew. Chem. Int. Ed.* **2012**, *51*, 2088–2092; *Angew. Chem.* **2012**, *124*, 2130–2134; b) H.-Q. Peng, J.-F. Xu, Y.-Z. Chen, L.-Z. Wu, C.-H. Tung, Q.-Z. Yang, *Chem. Commun.* **2014**, *50*, 1334–1337; c) P. Parkinson, C. E. I. Knappke, N. Kamonsutthipaijit, K. Sirithip, J. D. Matichak, H. L. Anderson, L. M. Herz, *J. Am. Chem. Soc.* **2014**, *136*, 8217–8220; d) H.-Q. Peng, L.-Y. Niu, Y.-Z. Chen, L.-Z. Wu, C.-H. Tung, Q.-Z. Yang, *Chem. Rev.* **2015**, *115*, 7502–7542; e) G. Chadha, Q.-Z. Yang, Y. Zhao, *Chem. Commun.* **2015**, *51*, 12939–12942.

[9] a) Y. X. Tian, R. Camacho, D. Thomsson, M. Reus, A. R. Holzwarth, I. G. Scheblykin, *J. Am. Chem. Soc.* **2011**, *133*, 17192–17199; b) J. Dostál, T. Mancal, R. Augulis, F. Vacha, J. Psencik, D. Zigmantas, *J. Am. Chem. Soc.* **2012**, *134*, 11611–11617; c) G. S. Orf, R. E. Blankenship, *Photosynth. Res.* **2013**, *116*, 315–331; d) J. Huh, S. K. Saikin, J. C. Brookes, S. Valleau, T. Fujita, A. Aspuru-Guzik, *J. Am. Chem. Soc.* **2014**, *136*, 2048–2057.

[10] a) C. Röger, Y. Miloslavina, D. Brunner, A. R. Holzwarth, F. Würthner, *J. Am. Chem. Soc.* **2008**, *130*, 5929–5939; b) J.

Szmytkowski, J. Conradt, H. Kuhn, C. M. Reddy, M. C. Balaban, T. S. Balaban, H. Kalt, *J. Phys. Chem. C* **2011**, *115*, 8832–8839; c) S. Furumaki, F. Vacha, S. Hirata, M. Vacha, *Acs Nano* **2014**, *8*, 2176–2182.

[11] a) Q. H. Cui, Y. S. Zhao, J. N. Yao, *Adv. Mater.* **2014**, *26*, 6852–6870; b) X. Wang, Q. Liao, Q. Kong, Y. Zhang, Z. Xu, X. Lu, H. Fu, *Angew. Chem. Int. Ed.* **2014**, *53*, 5863–5867; *Angew. Chem.* **2014**, *126*, 5973–5977.

[12] X. Zhang, X. Zhang, W. Shi, X. Meng, C. Lee, S. Lee, *Angew. Chem. Int. Ed.* **2007**, *46*, 1525–1528; *Angew. Chem.* **2007**, *119*, 1547–1550.

[13] a) D. M. Eisele, J. Knoester, S. Kirstein, J. P. Rabe, D. A. Vanden Bout, *Nat. Nanotechnol.* **2009**, *4*, 658–663; b) G. D. Scholes, T. Mirkovic, D. B. Turner, F. Fassioli, A. Buchleitner, *Energy Environ. Sci.* **2012**, *5*, 9374–9393; c) A. T. Haedler, K. Kreger, A. Issac, B. Wittmann, M. Kivala, N. Hammer, J. Kohler, H.-W. Schmidt, R. Hildner, *Nature* **2015**, *523*, 196–199; d) X. He, G. Zhu, J. Yang, H. Chang, Q. Meng, H. Zhao, X. Zhou, S. Yue, Z. Wang, J. Shi, L. Gu, D. Yan, Y. Weng, *Sci. Rep.* **2015**, *5*, 17076; e) J. Sung, P. Kim, B. Fimmel, F. Würthner, D. Kim, *Nat. Commun.* **2015**, *6*, 8646.

[14] a) G. Zumofen, A. Blumen, *Chem. Phys. Lett.* **1982**, *88*, 63–67; b) A. Krüger, C. Kryschi, L. Valkunas, D. Schmid, *Chem. Phys.* **1991**, *157*, 243–251; c) E. E. Nesterov, Z. G. Zhu, T. M. Swager, *J. Am. Chem. Soc.* **2005**, *127*, 10083–10088; d) V. A. Montes, G. V. Zyryanov, E. Danilov, N. Agarwal, M. A. Palacios, P. Anzenbacher, *J. Am. Chem. Soc.* **2009**, *131*, 1787–1795; e) H. Z. Lin, R. Camacho, Y. X. Tian, T. E. Kaiser, F. Würthner, I. G. Scheblykin, *Nano Lett.* **2010**, *10*, 620–626; f) X. Li, M. Bird, G. Mauro, S. Asaoka, A. R. Cook, H. C. Chen, J. R. Miller, *J. Phys. Chem. B* **2015**, *119*, 7210–7218.

[15] a) Y. X. Weng, K. C. Chan, B. C. Tzeng, C. M. Che, *J. Chem. Phys.* **1998**, *109*, 5948–5956; b) P. C. Mao, Z. Wang, W. Dang, Y. X. Weng, *Rev. Sci. Instrum.* **2015**, *86*, 123113.

Received: November 12, 2015